

Article

Improved Mechanical Properties of Cement-Stabilized Soft Clay Using Garnet Residues and Tire-Derived Aggregates for Subgrade Applications

Patimapon Sukmak ^{1,*}, Gampanart Sukmak ¹, Suksun Horpibulsuk ^{2,3}, Sippakarn Kassawat ⁴, Apichat Suddeepong ⁵ and Arul Arulrajah ⁶

- ¹ School of Engineering, Technology and Center of Excellence in Sustainable Disaster Management, Walailak University, Nakhonsithammarat 80161, Thailand; gampanart.su@wu.ac.th
- ² School of Civil Engineering, and Center of Excellence in Innovation for Sustainable Infrastructure Development, Suranaree University of Technology, Nakhon Ratchasima 30000, Thailand; suksun@g.sut.ac.th
- ³ Academy of Science, Royal Society of Thailand, Bangkok 10300, Thailand
- ⁴ Faculty of Commerce and Management, Prince of Songkla University, Trang Campus, Trang 92000, Thailand; sippakarn.k@psu.ac.th
- ⁵ School of Civil and Infrastructure Engineering, and Center of Excellence in Innovation for Sustainable Infrastructure Development, Suranaree University of Technology, Nakhon Ratchasima 30000, Thailand; suddeepong@g.sut.ac.th
- ⁶ Department of Civil and Construction Engineering, Swinburne University of Technology, Melbourne, VIC 3000, Australia; aarulrajah@swin.edu.au
- * Correspondence: patimapon.su@wu.ac.th; Tel.: +66-7567-3000



Citation: Sukmak, P.; Sukmak, G.; Horpibulsuk, S.; Kassawat, S.; Suddeepong, A.; Arulrajah, A. Improved Mechanical Properties of Cement-Stabilized Soft Clay Using Garnet Residues and Tire-Derived Aggregates for Subgrade Applications. *Sustainability* **2021**, *13*, 11692. <https://doi.org/10.3390/su132111692>

Academic Editor: Castorina Silva Vieira

Received: 21 September 2021
Accepted: 20 October 2021
Published: 22 October 2021

Publisher's Note: MDPI stays neutral with regard to jurisdictional claims in published maps and institutional affiliations.



Copyright: © 2021 by the authors. Licensee MDPI, Basel, Switzerland. This article is an open access article distributed under the terms and conditions of the Creative Commons Attribution (CC BY) license (<https://creativecommons.org/licenses/by/4.0/>).

Abstract: The growth of the global economy in recent years has resulted in an increase in infrastructure projects worldwide and consequently, this has led to an increase in the quantity of waste generated. Two recycled materials, namely garnet residues (GR) and tire-derived aggregates (TDA), were used to improve mechanical properties of soft clay (SC) subgrade in this study. GR was evaluated as a replacement material in SC prior to Type I Portland cement stabilization. TDA was also studied as an elastic material in cement-stabilized SC-GR. The laboratory tests on the cement-TDA-stabilized SC-GR included unconfined compressive strength (UCS), indirect tensile stress (ITS) and indirect tensile fatigue (ITF). Microstructural analysis on the cement-TDA-stabilized SC-GR was also performed to illustrate the role of GR and TDA contents on the degree of hydration. The UCS of cement-stabilized SC-GR increased when cement content increased from 0% to 2%. Beyond 2% cement content, the UCS development was slightly slower, possibly due to the presence of insufficient water for hydration. The GR reduces the specific surface and particle contacts of the SC-GR blends to be bonded with cementitious products. The optimum SC:GR providing the highest UCS was found to be 90:10 for all cement contents. Increased amounts of GR led to a reduction in UCS values due to its high water absorption, resulting in the insufficient water for the cement hydration. Moreover, the excessive GR replacement ratio weakened the interparticle bond strength due to its smooth and round particles. The TDA addition can enhance the fatigue resistance of the cement-stabilized SC-GR. The maximum fatigue life was found at 2% TDA content. The excessive TDA caused large amounts of micro-cracks in cement-TDA-stabilized SC-GR due to the low adhesion property of TDA. The SC:GR = 90:10, cement content = 2% and TDA content = 2% were suggested as the optimum ingredients. The outcome of this research will promote the usage of GR and TDA to develop a green high-fatigue-resistant subgrade material.

Keywords: soil-cement; pavement geotechnics; ground improvement; recycled waste; fatigue life; subgrade; compressive strength

1. Introduction

The continuous growth of emerging and developed economies has led to an increase in infrastructure projects, such as roads. Nakhon Si Thammarat is one of the largest

economic cities in the southern region of Thailand and most of its population lives in coastal areas. These coastal areas are underlain by soft clay (SC) deposits with high organic matter contents and with poor geotechnical properties which are also sensitive to moisture change [1,2]. Therefore, ground improvement is normally required before the construction of highway and road projects.

A widely accepted soft ground improvement technique is chemical stabilization using Portland cement, calcium carbide, quicklime and geopolymer [1,3–7]. In the past century, cement has been extensively acceptable for pavement and road construction. However, cement production releases a large amount of carbon dioxide (CO₂), which is a critical cause of global warming issues. Therefore, the usage of low CO₂ emission cementing agents with an alternative method for ground improvement is an interesting issue in research and development in transportation geotechnics.

In the past few years, the coarse and fine waste aggregates from civil engineering projects and/or industries, e.g., recycled concrete aggregates, crushed masonry bricks, recycled glasses and melamine debris, have been successfully utilized for ground improvement projects [8–15]. These recycled materials are low in plastic and have potential for improving the stiffness and strength of soil, especially clayey soil.

Due to the rapid growth of the global economy, marine and land transportation and oil demand have been increasing. This causes the increased quantity of wastes from repair and maintenance industries, namely garnet residues (GR) and tire-derived aggregates (TDA) (Figure 1). Garnet refers to the most complex crystalline silicate structure group with various chemical compositions. GR is a waste generated from usage of garnet in restored applications such as pre-finishing surface preparation before paint or other coatings on ship structures [16]. GR causes a major environmental concern worldwide, including in Thailand. In 2019, the total estimated global production of raw garnets for industrial purposes was 1.2 million tonnes/year, and China, USA, India, South Africa and Australia were the major producers. The consumption of raw garnets in 2020 in the USA was a 32% increase from that of 2016 [17]. In Thailand, the quantity of raw garnets acquired from both local and foreign sources for the domestic industries is about 8000 tonnes annually, which is mainly imported by the Thai Beverage Distribution Co., Ltd. (TBD). The global consumption of raw garnets forecasted indicates that these numbers will continue to increase annually [18]. The contaminants in GR consist of old paint, oil and other residues from the surface during blasting. GR is mostly disposed of at landfills. These wastes could disrupt the balance of the natural environment system through the pollution of water sources caused by runoff or flooding in the landfills. Kunchariyakun and Sukmak [19] undertook research to reduce pollution and reported that mixing GR with cement reduced leaching of heavy metals. Therefore, the reuse of GR in civil infrastructure applications is an interesting issue.



Figure 1. Waste rubber tires.

Recently, several researchers [19–24] employed GR as a fine aggregate in an infrastructure construction. The replacement of GR in natural river sand of up to a maximum of 25% could produce geopolymers that meet the required performance [21]. For road applications, GR can be used as a fine aggregate in asphalt concrete; the asphalt concrete with up to 25% GR replacement by weight of total aggregate had suitable Marshall properties comparable with conventional asphalt concrete using 100% granite aggregate [24]. Moreover, the GR replacement could improve California bearing ratio (CBR) of clayey sand for subgrade applications [23].

Automotive and truck tires and vulcanized rubbers have low elasticity and yield strain as well as high Young's modulus. Tires are made through the vulcanization process to form a crosslinked formation in the molecular structure of rubber to have high shear and temperature resistance for extreme environmental conditions. About one billion tonnes of TDA are generated annually around the world due to an increased number of vehicles [25]. TDA is a non-biodegradable material with a low degradation rate. Although the landfilling and combustion of TDA are a simple management technique, they cause recontamination of hazardous gases and dust in the atmosphere and underground water resources [25]. In past decades, the usage of TDA in road applications has become popular [26–28]. TDA as a fine aggregate in coarse recycled aggregates reduced the stiffness of concrete pavements; however, in turn, it could improve their performance, e.g., ductility and cracking and fatigue resistance. Moreover, the TDA could be used as an aggregate to improve geotechnical properties of highly expansive clay for subgrade applications [29]. The maximum unconfined compressive strength (UCS) and toughness were obtained at a 5% TDA replacement ratio. The higher TDA replacement ratio (>5%) caused a decrease in UCS. The swelling strain of expansive soil could also be minimized with the TDA replacement.

To the best of the authors' knowledge, there is no available research on the usage of combined GR and TDA in the mechanical strength improvement of soft clay to be a stabilized subgrade material. This research examined the feasibility of using GR as a replacement material in SC to improve its basic properties prior to cement stabilization to develop a green subgrade. TDA was used to improve the fatigue resistance of cement-stabilized SC–GR blends. The UCS, indirect tensile stress (ITS) and indirect tensile fatigue (ITF) of the cement–TDA-stabilized SC–GR were examined at various factors of SC:GR ratios and cement and TDA contents. Furthermore, the microstructural analysis was performed by using scanning electron microscopy and energy dispersive X-ray spectroscopy (SEM-EDX) to illustrate the role of GR in the interparticle bond strength improvement and TDA in the fatigue resistance improvement. Based on the authors' best knowledge, the investigation of cement–TDA-stabilized SC–GR blends under static and repeated tensile loading as well as their microstructural analysis has not been available, which is significant for road analysis and design. The outcome of this research will promote the usage of TDA and GR in road subgrade applications.

2. Materials and Methods

2.1. Materials

Tire derived-aggregates (TDA) was obtained from Union Commercial Development Co., Ltd., in Thailand, and air-dried before being used. The morphology and particle size distribution are shown in Figures 2a and 3, respectively. The TDA shape was irregular and prepared to have various single sizes of 2.830 mm, 2.000 mm, 0.841 mm, 0.595 mm, 0.400 mm, 0.297 mm and 0.250 mm. The TDA was then trial mixed to meet the gradation requirement for fine aggregates in accordance with ASTM C33/C33M-18 [30] (Figure 3). Table 1 presents the physical properties of TDA, indicating that the specific gravity and water absorption of TDA (ASTM C128-15 [31]) were 1.78% and 2.4%, respectively.

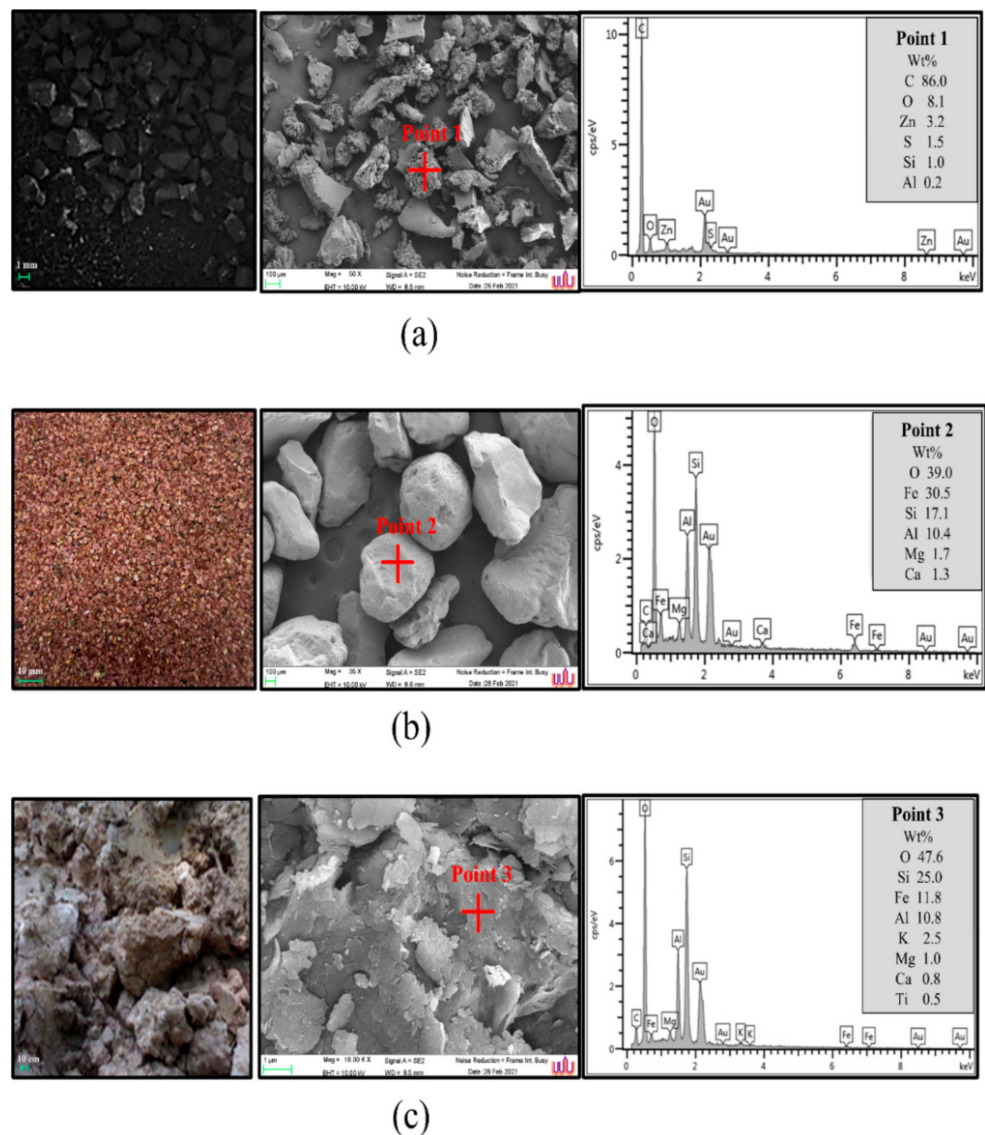


Figure 2. Appearance particles and SEM images of (a) tire-derived aggregates (TDA), (b) garnet residues (GR) and (c) soft clay (SC).

GR was sourced from Best Performance Engineering Co., Ltd. located in the south of Thailand; it came from the blasting and pre-finishing surface processes of ship and/or oil drilling tools. The GR was transferred to a laboratory and kept in sealed plastic bags for geotechnical tests. The physical properties, morphology and particle distribution curve are shown in Table 1 and Figures 2b and 3, respectively. The GR particles were relatively round in shape. The specific gravity and water absorption according to ASTM C128-15 [31] were 3.8% and 10.2%, respectively. The natural water content was approximately 0.2% based on ASTM D2216-19 [32]. GR has no liquid or plastic limits [33] due to its low plasticity. Based on ASTM C33/C33M-18 [30], the median diameter (D_{50}) of GR was 0.75 mm, similar to that of natural sand, as shown in Figure 3, whereas the specific gravity value of GR (=3.8) was greater than that of the natural sand (=2.7). The coefficient of uniformity (C_u) was 2.18 and the coefficient of curvature (C_c) was 1.35. The GR was therefore classified as poorly graded sand (SP) according to the Unified Soil Classification System (USCS) [34].

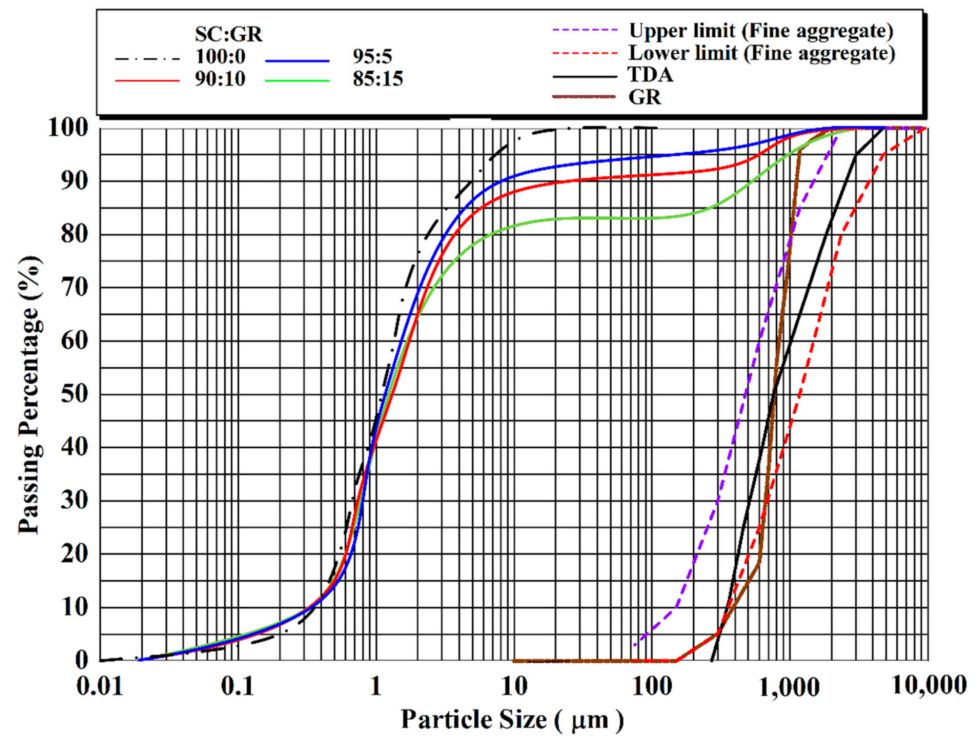


Figure 3. Gradation curves of GR and SC blends at SC:GR = 100:0, 95:5, 90:10 and 85:15.

Table 1. Physical properties of SC, GR and TDA.

Physical Properties	SC	GR	TDA
Specific gravity, SG	2.60	3.8	1.78
Water absorption (%)	-	10.2	2.4
Natural water content (%)	41.6	0.2	-
Liquid limit, LL (%)	65	N/A	-
Plastic limit, PL (%)	27.7	Non-plastic	-
Plastic index, PI (%)	37.3	N/A	-
Sand content (%)	-	100	-
Silt content (%)	25	-	-
Clay content (%)	78	-	-
D ₆₀ (mm)	-	0.95	1.01
D ₅₀ (mm)	-	0.75	0.75
D ₃₀ (mm)	-	0.52	0.52
D ₁₀ (mm)	-	0.29	0.35
C _u	-	2.18	2.88
C _c	-	1.35	0.76
Classification—USCS [34]	CH	SP	-
Classification—AASHTO [35]	A-7-6	A-1-b	-
Maximum dry unit weight, $\gamma_{d,max}$ (kN/m ³) [36]	15.4	-	-
Optimum moisture content, OMC (%)	23.7	-	-

Soft clay (SC) samples studied were alluvial clay commonly found in the Pak-Phanang estuary, in Nakhon Si Thammarat, Thailand. It was taken from a depth of 3–4 m below ground level. The morphology of SC particles was found to be irregular in shape (Figure 2c). Table 1 presents physical properties of SC, indicating that the specific gravity (ASTM D854 [37]), natural water content (ASTM D2216-19 [32]) and liquid limit and plastic limit (ASTM C4318-10 [33]) were 2.60%, 41.6%, 65% and 27.7%, respectively. The particle size distribution of SC is also shown in Figure 3. The SC was classified as high plasticity (CH) according to USCS [34]. The maximum dry unit weight ($\gamma_{d,max}$) and optimum

moisture content (OMC) of SC according to ASTM D 1557 [36] were 17.0 kN/m³ and 19.8%, respectively.

The chemical compositions of TDA, GR and SC were examined under a scanning electron microscope with energy dispersive X-ray spectroscopy (SEM/EDX) and are shown in Figure 2. The major cation elements in GR and SC were Si, Al and Fe, whereas C was the domain cation element in TDA.

2.2. Mix Proportions and Preparation

GR was blended with SC at SC:GR ratios of 100:0 (only soft clay), 95:5, 90:10 and 85:15 to improve the basic properties and compactability. GR replacement is undertaken to reduce the specific surface of the SC to improve the UCS of cement-stabilized SC. However, with high water absorption, the excess GR replacement ratio might cause a negative contribution. As such, the SC:GR ratio was limited to 85:15 in this study. Type I Portland cement was employed to stabilize the SC–GR blends at five different cement contents of 0%, 1%, 2%, 3% 4% and 5% by the dry weight of the SC–GR blends. The mixture was compacted under modified Proctor energy [37] to determine the $\gamma_{d,max}$ and OMC.

The cement–SC–GR blends of each ingredient were thoroughly mixed at the OMC until the homogenous mixture was achieved. The blends were compacted in a metal cylindrical mold with dimensions of 102 mm in diameter and 116.4 mm in height in five layers [37]. After 24 h, the cylindrical specimens were dismantled and sealed in plastic wraps to prevent evaporation. The cement-stabilized SC–GR specimens were kept at an ambient room temperature (27–30 °C) until the lapse of seven days of curing. The UCS tests were run on the cement-stabilized SC–GR specimens according to ASTM D1633 [38] to obtain the optimum of SC:GR ratio (highest UCS).

The TDA was blended with SC and GR at 1%, 2% and 3% by weight of the SC–GR mixtures at the optimum SC:GR ratio. The cement–SC–GR–TDA blends were then prepared at the OMC and compacted under modified Proctor energy to achieve the $\gamma_{d,max}$ state in a metal cylindrical mold with dimensions of 102 mm in diameter and 116.4 mm in height for UCS tests and in a metallic mold with dimensions of 101.60 mm diameter and 65.00 mm height for ITS and ITF tests. The specimens were dismantled, sealed in plastic wraps and kept at an ambient room temperature (27–30 °C) for seven days prior to the UCS, ITS, ITF and SEM-EDX testing. Figure 4 summarizes the steps of specimen preparation of cement–TDA-stabilized SC–GR specimens.

2.3. Testing Methods

2.3.1. Unconfined Compression Strength Test

The UCS tests were run according to ASTM D1633 [38] on the cement-stabilized SC–GR specimens with and without the TDA after seven days of curing, at a deformation rate of 1 mm/min. The UCS test was conducted on least five specimens to ensure testing consistency.

2.3.2. Indirect Tensile Strength Test

The indirect tensile strength (ITS) test in accordance with ASTM D6931 is performed to measure the tensile strength of pavement material for highway engineering design [39]. The ITS tests on cement–TDA-stabilized SC–GR specimens were conducted using a universal testing machine with a loading strip of 19 mm wide and 125 mm long at a deformation rate of 1 mm/min. According to the elastic theoretical approach, the ITS was calculated by using the following equation:

$$ITS = \frac{2P}{\pi DL} \quad (1)$$

where P is the is a maximum load (N), D is the specimen diameter (mm) and L is the specimen length (mm).

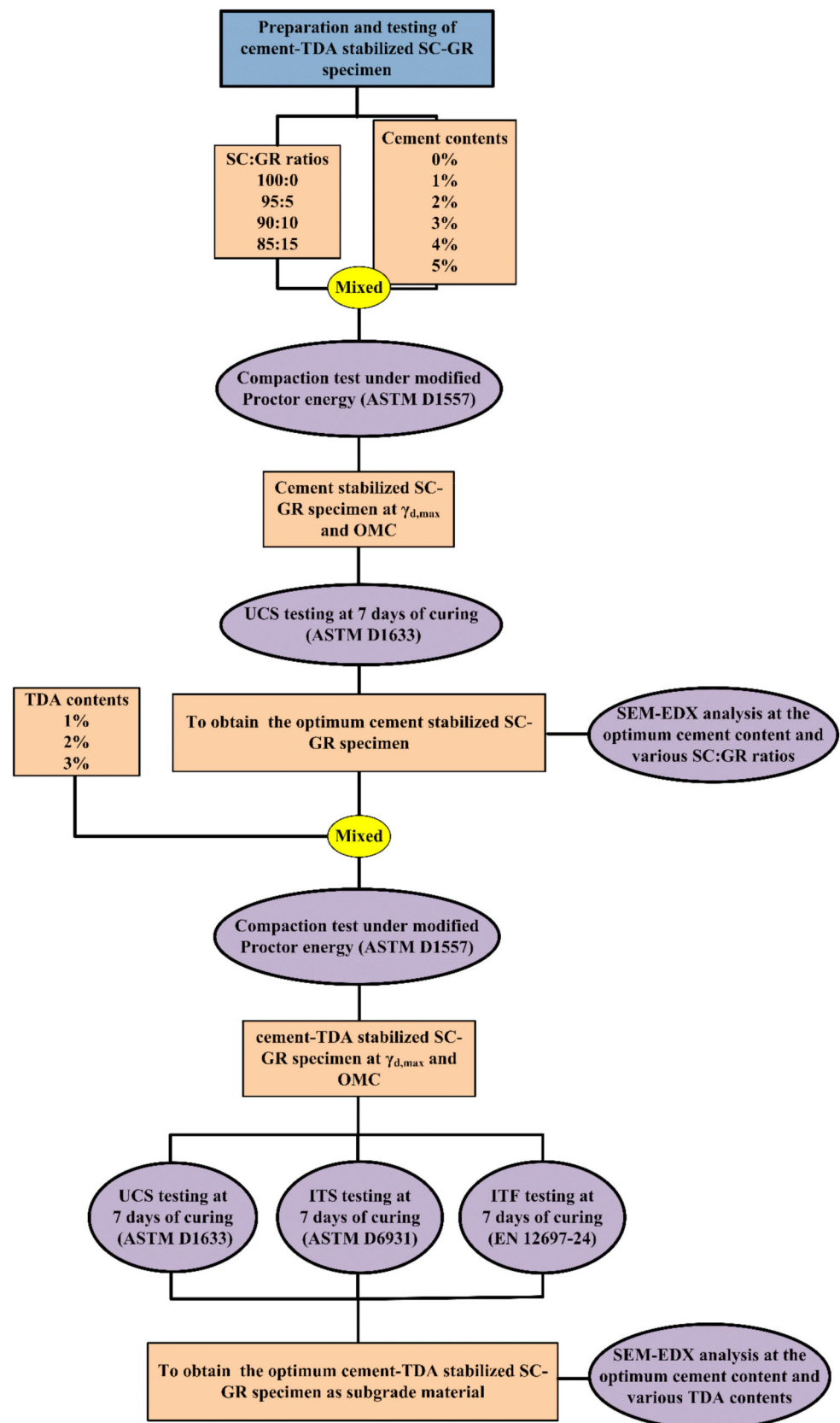


Figure 4. Summary of preparation and testing of cement–TDA-stabilized SC–GR specimens.

2.3.3. Indirect Tensile Fatigue Test

The indirect tensile fatigue (ITF) test according to EN 12697-24 is performed on road materials under controlled loading to examine the fatigue characterization. Kavussi and Modarres [40] recommended a loading frequency for the simulation of low traffic volume on rural roads of 0.66 Hz. Since rural roads are subject to the transportation of agricultural products such as livestock and agricultural products, which are relatively heavy, the applied stress level for the ITF specimens in this study was 80% of the corresponding ultimate ITS. The fatigue life of the ITF specimens is defined as the total number of loading cycles needed to damage the specimens. A linear variable differential transformer (LVDT) with an automatic recorder was used to measure horizontal deformations.

2.3.4. Scanning Electron Microscopy and Energy Dispersive X-ray Spectroscopy

The scanning electron microscopy and energy dispersive X-ray spectroscopy (SEM-EDX) analysis was achieved using a Merlin machine of Carl Zeiss, a company in Oberkochen, Germany, together with the Oxford Instruments Nano Analysis and the newest analytical system from Wycombe, U.K. The SEM-EDX specimen was a small fragment of the broken UCS specimen. It was frozen at $-195\text{ }^{\circ}\text{C}$ for five minutes in liquid nitrogen and evacuated at a pressure of 0.5 Pa at $-40\text{ }^{\circ}\text{C}$ to stop the hydration of cement. After drying, the SEM-EDX specimens were coated with gold to investigate the cementitious products and identify their chemical characterization by using the area mapping technique.

3. Results and Discussion

3.1. Cement-Stabilized SC–GR Blends

It is evident from Table 2 and Figure 3 that the basic properties of the SC–GR blends at SC:GR = 100:0, 95:5, 90:10 and 85:15, such as gradations and Atterberg limits, did not pass the requirements of the Thailand Department of Highways for stabilized base and subbase materials [41,42]. The SC–GR blends can only be used as stabilized subgrade material and its 7-day UCS must be greater than the minimum requirement of 294 kPa [43].

Table 2. Basic and mechanical properties of the SC–GR blends.

Properties	SC: GR Ratio				Standard for Stabilized Subbase (DH-S206/2532)	Standard for Stabilized Base (DH-S204/2556)
	100:0	95:05	90:10	85:15	Value	
Largest particle size (mm)	0.014	2.36	2.36	2.36	≤ 50	≤ 50
Passed at a 2.0 mm sieve (%)	100 *	100 *	100 *	100 *	NS	≤ 70
Passed at a 0.075 mm sieve (%)	100 *	94 *	91 *	83 *	≤ 40	≤ 25
Liquid limit, LL (%)	65.0	64.7	64.2	64.1	≤ 40	≤ 40
Plastic limit, PL (%)	27.7	30.7	31.8	31.7	NS	NS
Plasticity index, PI (%)	37.3	34	32.4	32.4	≤ 20	≤ 15
Maximum dry unit weight, $\gamma_{d,max}$ (kN/m ³) (ASTM D 15557)	15.4	15.6	15.8	16	NS	NS
Optimum moisture content, OMC (%) (ASTM D 15557)	23.7	23.1	21.8	21.5	NS	NS
Unconfined compression strength, UCS (kPa)	80 *	96 *	100 *	90 *	> 689	> 1724
Axial stress at 0.6% strain (kPa)	22	26	42	59	NS	NS
Secant modulus, E_{sec} (MPa)	3.7	4.3	7.0	9.8	NS	NS

Note: NS = not specified. * Did not meet requirement.

The change in Atterberg limits with cement content showed the impact of cement content on the specimens' plasticity characteristics (see Tables 2 and 3). The increase in cement content reduced the LL for all SC:GR ratios, for example, from 65% to 60.3% for cement contents from 0% to 5% for SC:GR = 100:0. This is because of the change in the SC's structure from dispersed to a flocculated structure. The increase in the plastic limit, PL,

was caused by prominent flocculated structure and the development of cementation in the SC–GR structure [44,45].

Table 3. Basic and mechanical properties of the cement-stabilized SC–GR specimens.

Cement Content (%)	Properties	SC: GR Ratio			
		100:0	95:5	90:10	85:15
1	Liquid limit, LL (%)	64.1	63.6	63.4	63.1
	Plastic limit, PL (%)	28.6	31	31.5	31.9
	Plasticity index, PI (%)	35.5	32.6	31.9	31.2
	Maximum dry unit weight, $\gamma_{d,max}$ (kN/m ³)	16	16.2	16.4	16.6
	Optimum moisture content, OMC (%)	21.9	21.4	20.5	20
	Unconfined compression strength, UCS (kPa)	159	176	260	214
	Axial stress at 0.6% strain (kPa)	39	50	76	109
	Secant modulus, E_{sec} (MPa)	6.5	8.3	12.7	18.2
2	Liquid limit, LL (%)	62.3	61.8	61.5	61.2
	Plastic limit, PL (%)	29.6	31.2	31.5	31.8
	Plasticity index, PI (%)	32.7	30.6	30	29.4
	Maximum dry unit weight, $\gamma_{d,max}$ (kN/m ³)	16.2	16.6	17.1	17.4
	Optimum moisture content, OMC (%)	20.8	20.5	20.0	19.6
	Unconfined compression strength, UCS (kPa)	222	278	403	367
	Axial stress at 1% strain (kPa)	56	76	103	122
	Secant modulus, E_{sec} (MPa)	9.3	12.7	17.2	20.3
3	Liquid limit, LL (%)	61.1	60.7	60.4	60.2
	Plastic limit, PL (%)	30.1	32.1	32.6	33
	Plasticity index, PI (%)	31	28.6	27.8	27.2
	Maximum dry unit weight, $\gamma_{d,max}$ (kN/m ³)	16.8	17.2	17.3	17.5
	Optimum moisture content, OMC (%)	20.4	19.5	19.3	19
	Unconfined compression strength, UCS (kPa)	242	340	462	424
	Axial stress at 1% strain (kPa)	77	132	157	187
	Secant modulus, E_{sec} (MPa)	12.8	22.0	26.2	31.2
4	Liquid limit, LL (%)	60.3	59.7	59.5	59
	Plastic limit, PL (%)	31.6	33.8	34.1	34.8
	Plasticity index, PI (%)	28.7	25.9	25.4	24.2
	Maximum dry unit weight, $\gamma_{d,max}$ (kN/m ³)	17	17.4	17.9	18.1
	Optimum moisture content, OMC (%)	19.7	19.2	18.8	18.3
	Unconfined compression strength, UCS (kPa)	279	376	524	492
	Axial stress at 1% strain (kPa)	109	200	218	282
	Secant modulus, E_{sec} (MPa)	18.2	33.3	36.3	47.0
5	Liquid limit, LL (%)	60.3	59.7	59.5	59
	Plastic limit, PL (%)	33.2	33.8	35.7	34.8
	Plasticity index, PI (%)	27.1	25.9	23.8	24.2
	Maximum dry unit weight, $\gamma_{d,max}$ (kN/m ³)	17.2	17.8	18.2	18.4
	Optimum moisture content, OMC (%)	19.4	19	18.4	17.7
	Unconfined compression strength, UCS (kPa)	294	410	549	535
	Axial stress at 1% strain (kPa)	171	280	285	359
	Secant modulus, E_{sec} (MPa)	28.5	46.7	47.5	59.8

Table 2 and Figure 5 show the values of $\gamma_{d,max}$ and OMC and compaction curves, respectively, at SC:GR = 100:0, 95:5, 90:10 and 85:15 for various cement contents. For all SC:GR ratios, the addition of cement to the SC–GR blends increased the $\gamma_{d,max}$ but reduced the OMC, similar to the cement-stabilized coarse-grained soil [46] and the cement-stabilized fine-grained soil [44]. The cement had higher specific gravity than the SC; therefore, the density of the specimens increased when the cement content increased. The cement reaction mechanism consists of two stages: immediate and long-term reactions. In the immediate reaction, the Ca^{2+} ions from cement are adsorbed into negative charges of the SC surface and reduce the thickness of diffused double layers of the SC particles. The edge-to-face

contacts of SC particles, on the other hand, are increased [44,45], thus resulting in an increase in PL with a decrease in LL. The decrease in LL reduces the OMC and increases $\gamma_{d,max}$ [44].

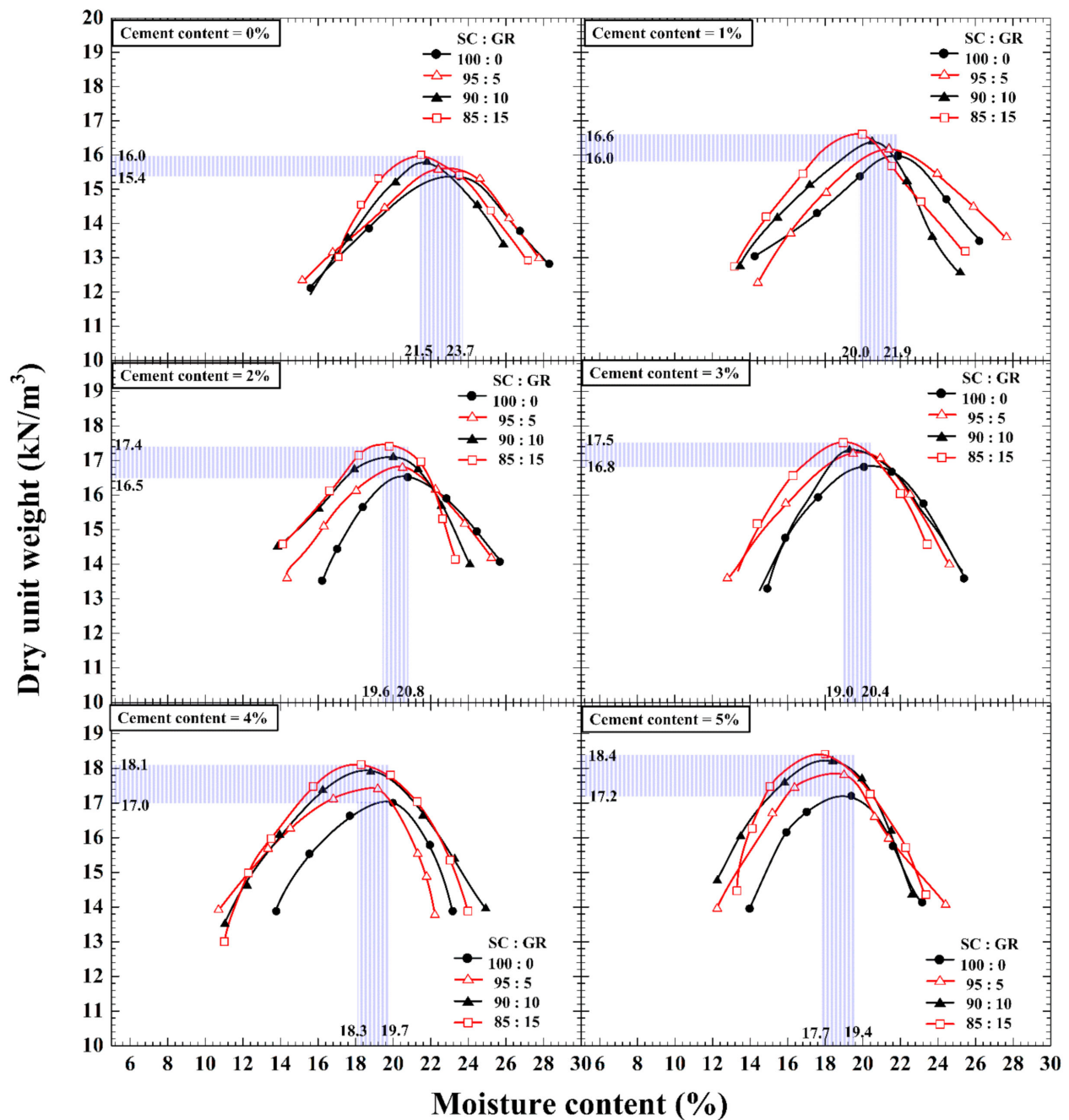


Figure 5. Dry unit weight versus moisture content curves of SC–GR blends with various cement contents.

For all cement contents, the $\gamma_{d,max}$ of the cement–SC–GR mixture increased with the increased GR because the specific gravity of GR was higher than that of SC and cement, as shown by the $\gamma_{d,max}$ of SC:GR = 100:0 being lower than the $\gamma_{d,max}$ of SC:GR = 85:15 for all cement contents. The increase in the $\gamma_{d,max}$ is associated with the decrease in the OMC, as presented in Figure 5.

Figure 6 shows stress–strain curves under the UCS tests for cement contents = 0 to 5% and SC:GR = 100:0 to 85:15. For all cement contents and SC:GR ratios tested, the cement-stabilized SC–GR specimens exhibited brittle behavior with a rapid drop in stress

after peak. Since the strain levels developed in road subgrade material due to traffic load varies from 0.003% to 0.6% [47], in this research the secant modulus (E_{sec}) was calculated at 0.6% strain to describe the stiffness of a material. The equation for calculating E_{sec} is:

$$E_{SEC} = \frac{\sigma_{a@0.6\% \text{ strain}} - \sigma_{a@0\% \text{ strain}}}{\varepsilon_{a@0.6\% \text{ strain}} - \varepsilon_{a@0\% \text{ strain}}} \quad (2)$$

where $\sigma_{a@0.6\% \text{ strain}}$ is the stress at 0.6% strain, $\sigma_{a@0\% \text{ strain}}$ is the stress at 0% strain (equal to 0), $\varepsilon_{a@0.6\% \text{ strain}}$ is the strain at 0.6% and $\varepsilon_{a@0\% \text{ strain}}$ is the strain at 0% (equal to 0).

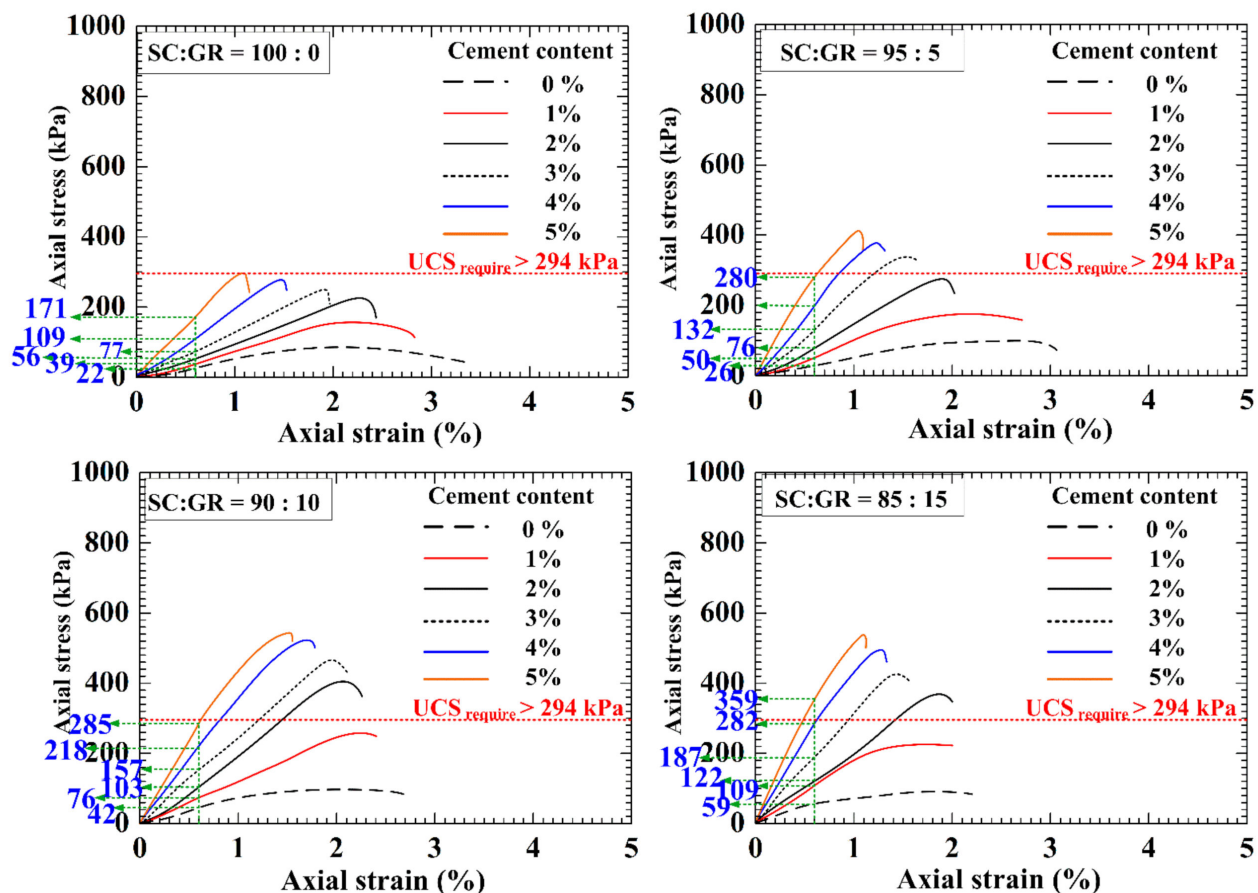


Figure 6. Stress–strain curves under UCS test for cement contents = 0–5% for various SC:GR ratios.

Table 3 shows the variation of E_{sec} of all cement-stabilized SC–GR specimens at 0.6% strain. The E_{sec} and UCS for all SC:GR ratios tended to increase with the increased cement content (Figure 6). Figure 7 shows the UCS development with the increased cement contents of the cement-stabilized SC–GR specimens. As the cement contents increased up to 2%, the cementation bonds at the contact points between the SC–GR particles were stronger due to predominant Calcium Silicate Hydrate (C-S-H, cementitious products). The amount of C-S-H products increased with an increase in the cement content. This range of cement contents could be termed as the active zone. When cement contents were between 2% and 5%, the UCS development was slightly slower, possibly because the water at OMC was not sufficient for hydration.

The role of GR is also clearly depicted in Figure 7. Without GR replacement, the UCS of cement-stabilized SC at cement contents = 1–5% could not meet the minimum requirement of 294 kPa. The UCS values at all cement contents were increased with the GR replacement ratio up to the optimum value of SC:GR = 90:10. This implies that the GR reduces the specific surface and particle contacts of the SC–GR blends to be bonded cementitious products, hence the stronger interparticle bond strength at the same input of cement.

However, when SC:GR > 90:10, the UCS decreased. The GR has high water absorption (refer to Table 1); the higher GR absorbed more water into its particles and therefore, the water is not sufficient cement hydration. Moreover, the excessive smooth and round GR particles caused the decrease in interparticle bond strength. The 2% cement content was found to be the most effective for the OMC when utilized with GR replacement. For all SC:GR ratios tested, the 2% cement-stabilized SC–GR blends met the strength requirement (UCS > 294.2 kPa) for stabilized subgrade specified by the DOH [43].

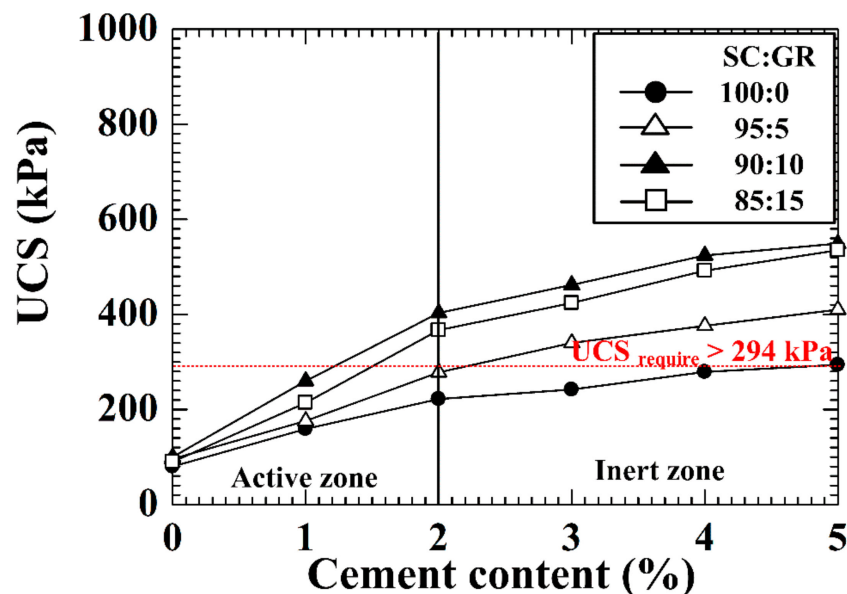


Figure 7. UCS development as a function of cement content.

Figure 8a,b show the SEM-EDX analyses of the specimen at cement content of 2% and SC:GR ratios of 90:10 and 85:15, respectively, to understand the role of GR replacement. The specimen at SC:GR = 90:10 had more C-S-H products (confirmed by EDX result in Area A) in pores than the specimens at SC:GR = 85:15. Moreover, the specimens at SC:GR = 85:15 had more micropores than the specimens at SC:GR = 85:15. The lower cementitious products in specimens at SC:GR = 85:15 were also confirmed by EDX results (refer to Area C (SC particles) and point B (GR particles)). These results confirmed the lower degree of cement hydration at the excessive GR replacement ratio (SC:GR = 85:15) due the high water absorption of GR particles, which resulted in lower strength and stiffness.

3.2. Cement–TDA–Stabilized SC–GR Blends

Figure 9 depicts dry unit weight versus moisture content relationship of the cement–TDA–SC–GR mixtures when SC:GR = 90:10 and cement content = 2% (optimum ingredient) with TDA contents. The $\gamma_{d,max}$ slightly reduced with an increase in the TDA content. Nonetheless, the OMC slightly increased with the increased TDA content (refer to Table 4). Figure 10 presents stress–strain curves under the UCS test when SC:GR = 90:10 and cement content = 2% for various TDA contents. The reduction in UCS and stiffness could be seen with an increase in the TDA content. Moreover, the TDA stabilization resulted in the increase in area under the curves and the decrease in E_{sec} , indicating the increased toughness and the energy absorption before rupture. This characteristic is associated with the higher fatigue resistance, which is required for durable roads. According to the UCS requirement, TDA > 2% cannot be accepted in practice.

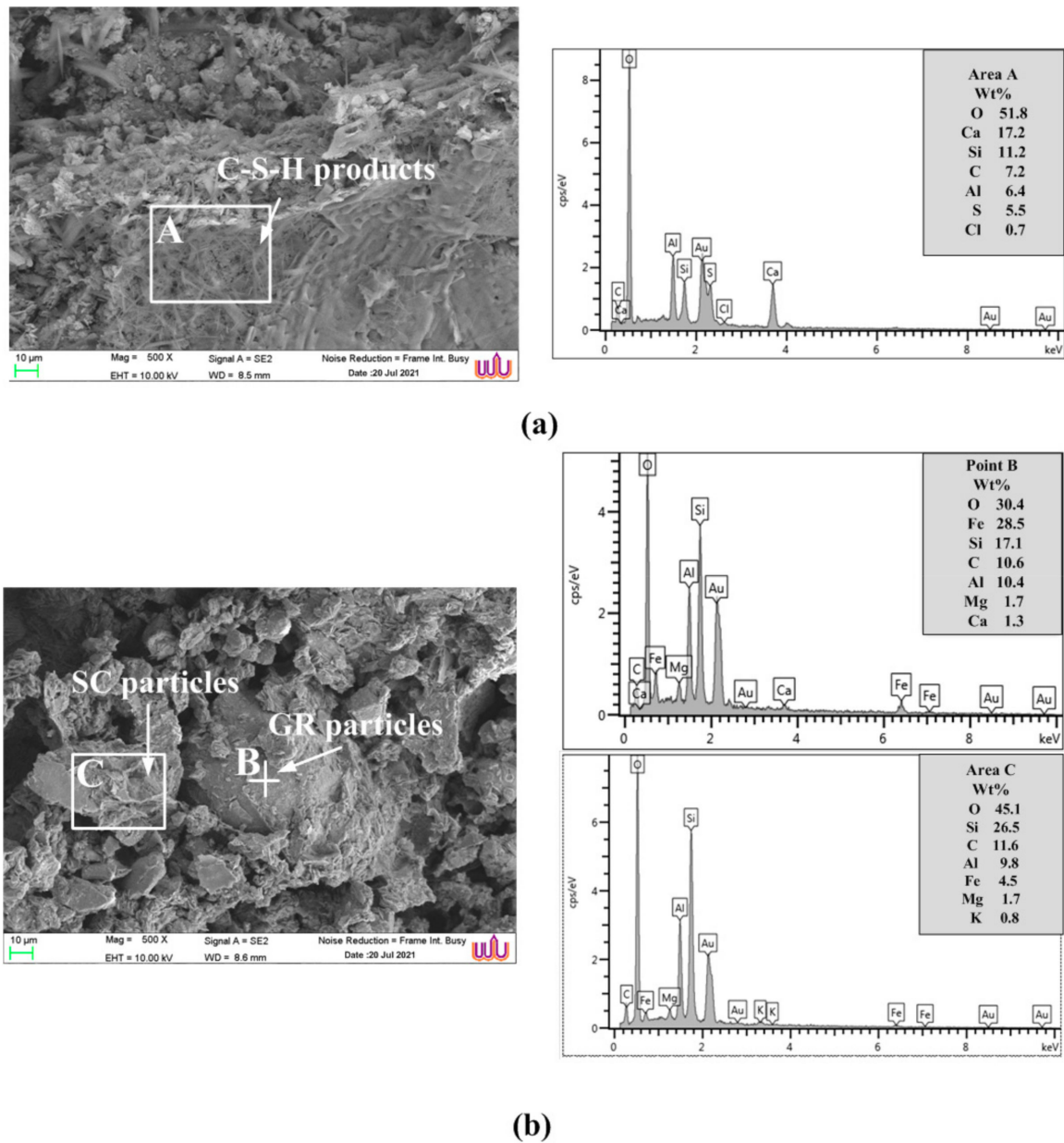


Figure 8. SEM-EDX analyses of specimens at cement content of 2% and when SC:GR ratio = (a) 90:10 and (b) 85:15.

Table 4. Basic and mechanical properties of the cement–TDA-stabilized SC–GR specimens when SC:GR ratio = 90:10 and cement content = 2% with various TDA contents.

Cement Content (%)	Properties	TDA Content (%)			
		0	1	2	3
2	Maximum dry unit weight, $\gamma_{d,max}$ (kN/m ³)	17.1	16.8	16.6	16.2
	Optimum moisture content, OMC (%)	20.0	21.3	22.0	22.5
	Unconfined compression strength, UCS (kPa)	403	379	339	231
	Axial stress at 0.6% strain (kPa)	103	79	42	21
	Secant modulus, E_{sec} (MPa)	17.2	13.2	6.7	5.2
	Indirect tensile stress, ITS (kPa)	113.6	132.3	137.2	119.3
	Indirect Tensile Fatigue, N_f (pulses)	22	95	115	72
	Initial deformation, Δp (mm)	0.19	0.79	1.18	0.94

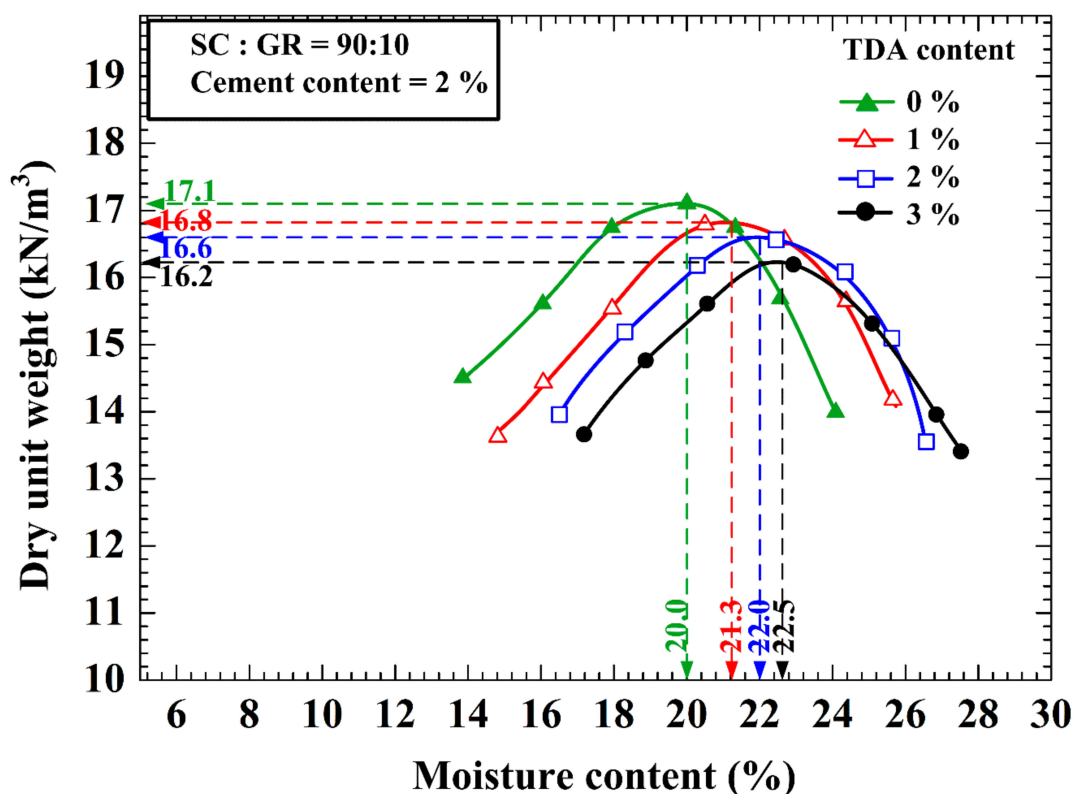


Figure 9. Dry unit weight versus moisture content relationship of cement-TDA-stabilized SC-GR mixtures when SC:GR = 90:10 and cement content = 2% with various TDA contents.

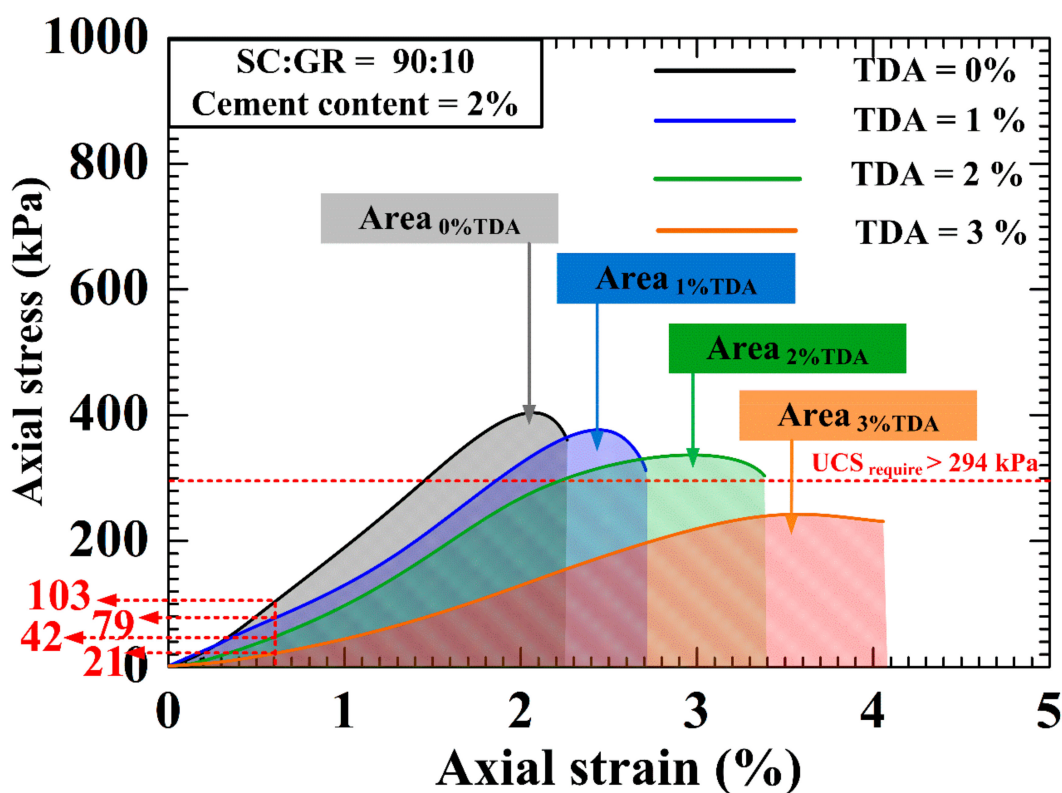


Figure 10. Stress-strain curves under the UCS test of cement-TDA-stabilized SC-GR mixtures when SC:GR = 90:10 and cement content = 2% for various TDA contents.

Figure 11a shows the relationship between the number of cycles versus horizontal deformation of the cement–TDA-stabilized SC–GR specimens when SC:GR = 90:10 and cement content = 2% for TDA contents of 0% to 3%. Figure 11b shows the typical relationship between the number of cycles versus horizontal deformation, which is divided into three zones. In the first zone, at a small number of cycles, high deformation occurred on the specimen because of the increase in plastic deformation. In the second zone, the increase in number of cycles is associated with the lower rate of deformation, whereby the micro-cracks are gradually formed and propagated. In the third zone, the complete splitting failure occurs because of the accumulated microcracks on specimen. Figure 11b also shows the method of determining fatigue life (N_f) and initial deformation in zone 2 (Δp). The initial deformation (Δp) is defined as the intersection of the straight lines extending from the linear portion in zone 1 and zone 2. The N_f is the number of cycles at the splitting failure of the specimen.

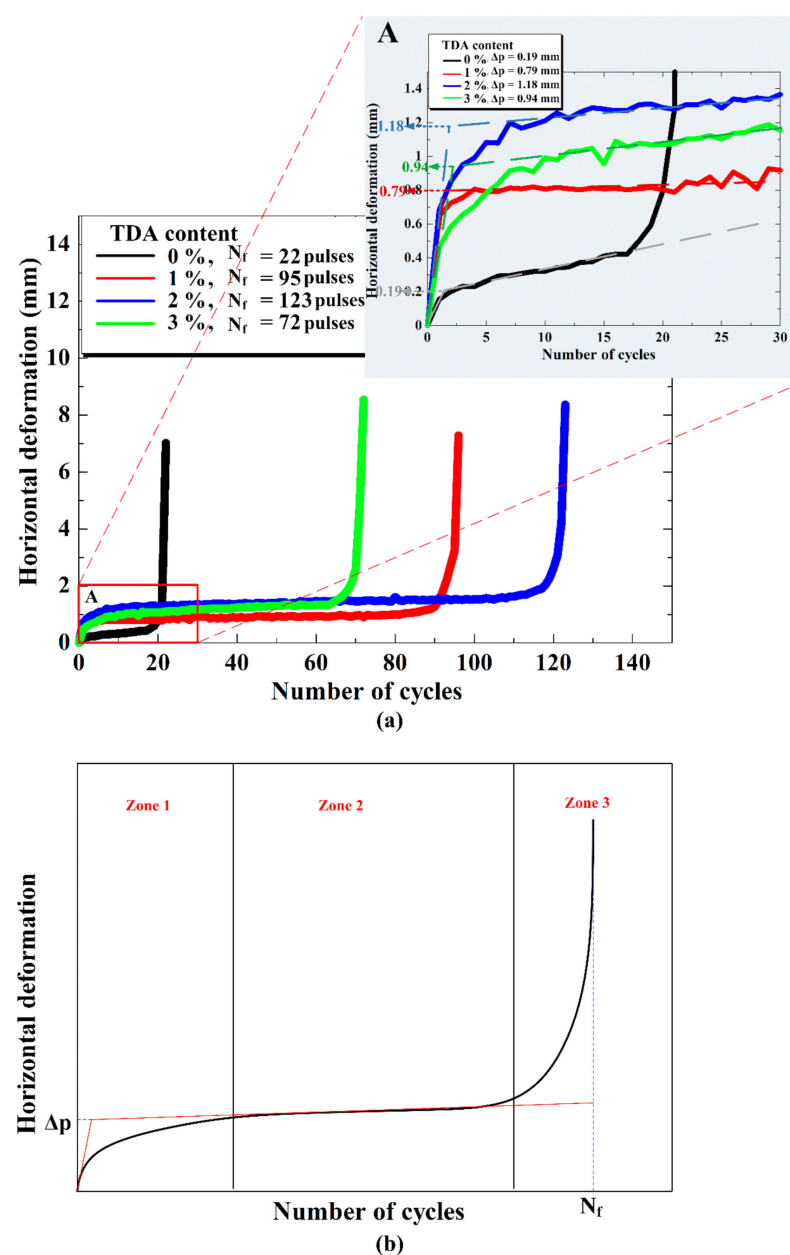


Figure 11. Relationship between the number of cycles versus horizontal deformation of (a) the cement–TDA-stabilized SC–GR specimen of SC:GR ratio = 90:10 and cement content = 2% and (b) the method of the determining of fatigue life (N_f) and initial deformation (Δp).

At zone 2, the cement–TDA-stabilized SC–GR specimens had longer N_f than the cement-stabilized SC–GR specimens (TDA = 0%). This indicated that the TDA improved the ductility behavior, whereas the specimen at TDA = 0% exhibited sudden failure. The Δp and N_f values increased with the TDA content up to the optimal TDA of 2%, after which they decreased. For example, the Δp values were increased from 0.19 to 1.18 mm for TDA contents from 0% to 2% and N_f values were increased from 22 to 123 pulses for TDA contents from 0% to 2%. The increase in both Δp and N_f is associated with the increase in ITS (Table 4). In other words, both Δp and N_f values are directly related to the ITS.

The role of TDA in the UCS and fatigue resistance can be explained by the SEM-EDX analyses shown in Figure 12. More C–S–H gels (Area E) bonding TDA (Area D) in SC–GR particles and in voids were observed at 1% TDA content (Figure 12a), when compared with 2% TDA content (Figure 12b) and 3% TDA content (Figure 12c). More micro-cracks within TDA–SC–GR clusters were, however, found (red dash line) for 2% and 3% TDA contents when compared with 1% TDA content. The cracks developed were attributed to the low adhesion property of TDA particles. As such, the UCS, which represents the static and short-term strength, decreased with increasing TDA content. Even with micro-cracks, the TDA particles at optimum content can absorb more cyclic load energy and result in larger N_f . However, the excessive TDA with more micro-cracks caused excessive plastic deformation and the reduction in energy absorption and hence, the reduction in N_f .

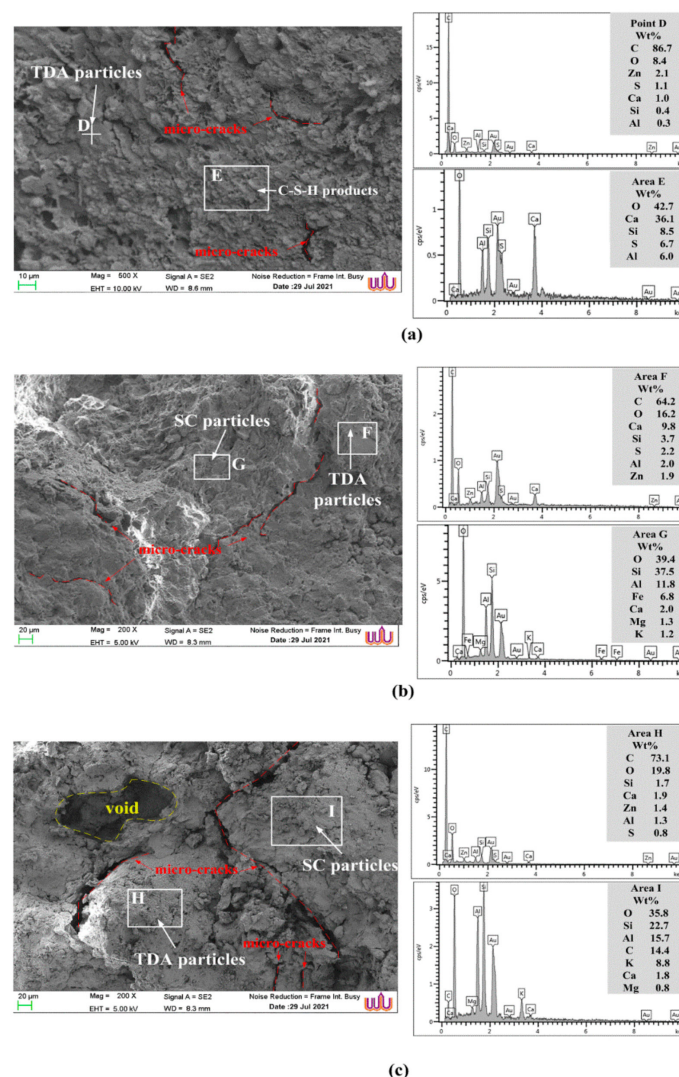


Figure 12. SEM-EDX analyses of the cement–TDA-stabilized SC–GR specimens when SC:GR ratio = 90:10 and cement content = 2%, and WRT content of (a) 1%, (b) 2% and (c) 3%.

3.3. Economic and Environmental Benefits

Table 5 shows the total construction costs of cement–TDA-stabilized SC–GR and lateritic soil as a pavement subgrade. The total construction cost of cement–TDA-stabilized SC–GR was 48.48% less than that of compacted lateral soil in 1 m³ highway, indicating the cost savings. Moreover, the industry could reduce the GR and TDA disposal costs by approximately 58.03 USD/tonne (from GMA Garnet Group) and 10 USD/tonne [48], respectively, and also reduce environmental pollution from disposal in landfills.

Table 5. Material costs comparison between of using cement, GR and TDA in SC and compacted lateral soil for subgrade application in 1 cubic meter.

Section	Material	Volume(m ³) ^a	Weight (kg)	Price (USD/m ³) ^b	Total Cost (USD)
Cement–TDA-stabilized SC–GR at SC:GR = 90:10, cement content = 2% and TDA content = 2%.	cement	0.02	63	5.09 [49]	5.11
	GR	0.096	364.8	-	
	TDA	0.02	35.6	0.0178 ^c	
	SC	0.864	2246.4	-	
Lateral soil	lateral soil	1	-	10.54 [49]	10.54

^a Based on the dry soil weight. ^b Not including shipping and labor costs. ^c The price from Union Commercial Development Co., Ltd., Samut Prakan, Thailand.

4. Conclusions

This research aims to examine the feasibility of using GR as a replacement material in soft clay (SC) prior to cement stabilization to be a subgrade material. TDA was used to improve the fatigue resistance of cement-stabilized SC–GR. The mechanical and microstructural investigation of the cement–TDA-stabilized SC–GR were performed to ascertain it as a sustainable subgrade material. The following conclusions can be drawn from this study.

1. The increase in $\gamma_{d,max}$ and the decrease in OMC were caused by changing the dispersed structure to a flocculated SC–GR structure with the addition of cement. Therefore, $\gamma_{d,max}$ increased with the GR replacement ratio. The GR replacement reduced the specific surface of SC, but at the same time, increased the water absorption. The optimum SC:GR ratio was found at 90:10. The 2% cement content for stabilized SC–GR at SC:GR of 90:10 was the optimum mixture.
2. The UCS and stiffness of cement-stabilized SC–GR were found to reduce with the increase in TDA content. This is due to the low adhesion property of TDA; the micro-cracks within SC–GR–TDA matrix were detected with the increased TDA content. However, the increased TDA content improved the ductile behavior and resulted in the increased energy absorption before rupture. The optimum TDA content was found to be 2%. When TDA content was greater than 2%, the excessive micro-cracks caused excessive plastic deformation and the reduction in energy absorption and, hence, the reduction in fatigue life.
3. The cement–TDA-stabilized SC–GR at SC:GR of 90:10, cement content of 2% and TDA content of 2% is suggested as a sustainable subgrade material. Its UCS met the strength requirements of the Department of Highways, Thailand (DH-S201/2532), and its fatigue life was found to be the highest when compared to other SC:GR ratios with the same cement content. The improved fatigue resistance of the cement-stabilized SC–GR is necessary for durable roads.

Author Contributions: Conceptualization, P.S., G.S., S.H., S.K., A.S. and A.A.; methodology, P.S.; formal analysis, P.S.; writing—original draft preparation, P.S.; writing—review and editing, S.H. and A.A.; supervision, S.H. and A.A.; funding acquisition, P.S. and S.H. All authors have read and agreed to the published version of the manuscript.

Funding: This research was supported by the new strategic research (P2P) project (grant no. CGS-P2P-2564-001), Walailak University, Thailand, and the National Science and Technology Development Agency under the Chair Professor Program (grant no. P-19-52303).

Institutional Review Board Statement: Not applicable.

Informed Consent Statement: Not applicable.

Data Availability Statement: The data presented in this study are available on request from the corresponding author. The data are not publicly available due to privacy restrictions.

Acknowledgments: The first author is grateful to a financial support from Walailak University. Facilities and equipment provided from the Walailak University are very much appreciated. The first and the third authors acknowledge the financial support from the new strategic research (P2P) project (grant no. CGS-P2P-2564-001), Walailak University, Thailand, and the National Science and Technology Development Agency under the Chair Professor Program (grant no. P-19-52303).

Conflicts of Interest: The authors declare no conflict of interest.

References

- Sukmak, P.; Sukmak, G.; Horpibulsuk, S.; Setkit, M.; Kassawat, S.; Arulrajah, A. Palm oil fuel ash-soft soil geopolymer for subgrade applications: Strength and microstructural evaluation. *Road Mater. Pavement Des.* **2019**, *20*, 110–131. [\[CrossRef\]](#)
- Du, Y.-J.; Jiang, N.-J.; Liu, S.-Y.; Horpibulsuk, S.; Arulrajah, A. Field evaluation of soft highway subgrade soil stabilized with calcium carbide residue. *Soils Found.* **2016**, *56*, 301–314. [\[CrossRef\]](#)
- Arulrajah, A.; Yaghoubi, M.; Disfani, M.M.; Horpibulsuk, S.; Bo, M.W.; Leong, M. Evaluation of fly ash-and slag-based geopolymers for the improvement of a soft marine clay by deep soil mixing. *Soils Found.* **2018**, *58*, 1358–1370. [\[CrossRef\]](#)
- Miura, N.; Horpibulsuk, S.; Nagaraj, T. Engineering behavior of cement stabilized clay at high water content. *Soils Found.* **2001**, *41*, 33–45. [\[CrossRef\]](#)
- Horpibulsuk, S.; Phetchuay, C.; Chinkulkijniwat, A. Soil stabilization by calcium carbide residue and fly ash. *J. Mater. Civil Eng.* **2012**, *24*, 184–193. [\[CrossRef\]](#)
- Dahal, B.K.; Zheng, J.-J.; Zhang, R.-J.; Song, D.-B. Enhancing the mechanical properties of marine clay using cement solidification. *Mar. Georesour. Geotechnol.* **2019**, *37*, 755–764. [\[CrossRef\]](#)
- Sukmak, P.; Horpibulsuk, S.; Shen, S.-L. Strength development in clay–fly ash geopolymer. *Construct. Build. Mater.* **2013**, *40*, 566–574. [\[CrossRef\]](#)
- Arulrajah, A.; Jegatheesan, P.; Bo, M.W.; Sivakugan, N. Geotechnical characteristics of recycled crushed brick blends for pavement sub-base applications. *Can. Geotech. J.* **2012**, *49*, 796–811. [\[CrossRef\]](#)
- Arulrajah, A.; Ali, M.M.Y.; Disfani, M.M.; Piratheepan, J.; Bo, M.W. Geotechnical performance of recycled glass-waste rock blends in footpath bases. *J. Mater. Civ. Eng.* **2013**, *25*, 653–661. [\[CrossRef\]](#)
- Arulrajah, A.; Piratheepan, J.; Disfani, M.M.; Bo, M.W. Geotechnical and geoenvironmental properties of recycled construction and demolition materials in pavement subbase applications. *J. Mater. Civ. Eng.* **2013**, *25*, 1077–1088. [\[CrossRef\]](#)
- Donrak, J.; Arulrajah, A.; Rachan, R.; Horpibulsuk, S. Improvement of marginal lateritic soil using melamine debris replacement for sustainable engineering fill materials. *J. Clean. Prod.* **2016**, *134*, 515–522. [\[CrossRef\]](#)
- Kianimehr, M.; Shourijeh, P.T.; Binesh, S.M.; Mohammadinia, A.; Arulrajah, A. Utilization of recycled concrete aggregates for light-stabilization of clay soils. *Construct. Build. Mater.* **2019**, *227*, 116792. [\[CrossRef\]](#)
- Naeini, M.; Mohammadinia, A.; Arulrajah, A.; Horpibulsuk, S.; Leong, M. Stiffness and strength characteristics of demolition waste, glass and plastics in railway capping layers. *Soils Found.* **2019**, *59*, 2238–2253. [\[CrossRef\]](#)
- Arulrajah, A.; Disfani, M.M.; Haghghi, H.; Mohammadinia, A.; Horpibulsuk, S. Modulus of rupture evaluation of cement stabilized recycled glass/recycled concrete aggregate blends. *Constr. Build. Mater.* **2015**, *84*, 146–155. [\[CrossRef\]](#)
- Yaowarat, T.; Horpibulsuk, S.; Arulrajah, A.; Maghool, F.; Mirzababaei, M.; Safuan, A.A.; Chinkulkijniwat, A.R. Cement stabilisation of recycled concrete aggregate modified with polyvinyl alcohol. *Int. J. Pavement Eng.* **2020**, 1–9. [\[CrossRef\]](#)
- Sidhardhan, S.; Sheela, S.J.; Meylin, J.S. Study on sea sand as a partial replacement for fine aggregate. *J. Adv. Chem.* **2017**, *13*, 6166–6171.
- Olson, D.W. Garnet, industrial. In *Minerals Yearbook Metals and Minerals*; Government of India: Nagpur, India, 2021; p. 1.
- Mines, I.B.O. *Indian Minerals Yearbook 2018 (Part-III: Mineral Reviews)*; Government of India, Ministry of Mines: Nagpur, India, 2018.
- Kunchariyakun, K.; Sukmak, P. Utilization of garnet residue in radiation shielding cement mortar. *Constr. Build. Mater.* **2020**, *262*, 120122. [\[CrossRef\]](#)
- Muttashar, H.L.; Bin Ali, N.; Ariffin, M.A.M.; Hussin, M.W. Microstructures and physical properties of waste garnets as a promising construction materials. *Case Stud. Constr. Mater.* **2018**, *8*, 87–96. [\[CrossRef\]](#)
- Muttashar, H.L.; Ariffin, M.A.M.; Hussein, M.N.; Hussin, M.W.; Bin Ishaq, S. Self-compacting geopolymer concrete with spend garnet as sand replacement. *J. Build. Eng.* **2018**, *15*, 85–94. [\[CrossRef\]](#)

22. Huseien, G.F.; Sam, A.R.M.; Shah, K.W.; Budiea, A.; Mirza, J. Utilizing spend garnets as sand replacement in alkali-activated mortars containing fly ash and GBFS. *Constr. Build. Mater.* **2019**, *225*, 132–145. [[CrossRef](#)]
23. Sani, N.M.; Mohamed, A.; Khalid, N.H.A.; Nor, H.M.; Hainin, M.R.; Giwangkara, G.G.; Hassan, N.A.; Kamarudin, N.A.S.; Mashros, N. Improvement of CBR value in soil subgrade using garnet waste. *IOP Conf. Ser. Mater. Sci. Eng.* **2019**, *527*, 012060. [[CrossRef](#)]
24. Aletba, S.R.; Hassan, N.; Aminudin, E.; Hussein, A.A.; Jaya, R. Marshall properties of asphalt mixture containing garnet waste. *Adv. Res. Mater. Sci.* **2018**, *43*, 22–27.
25. Thomas, B.S.; Gupta, R.C. A comprehensive review on the applications of waste tire rubber in cement concrete. *Renew. Sustain. Energy Rev.* **2016**, *54*, 1323–1333. [[CrossRef](#)]
26. Hernández-Olivares, F.; Barluenga, G.; Parga-Landa, B.; Bollati, M.; Witoszek, B. Fatigue behaviour of recycled tyre rubber-filled concrete and its implications in the design of rigid pavements. *Constr. Build. Mater.* **2007**, *21*, 1918–1927. [[CrossRef](#)]
27. Meddah, A.; Beddar, M.; Bali, A. Use of shredded rubber tire aggregates for roller compacted concrete pavement. *J. Clean. Prod.* **2014**, *72*, 187–192. [[CrossRef](#)]
28. Arulrajah, A.; Mohammadinia, A.; Maghool, F.; Horpibulsuk, S. Tyre derived aggregates and waste rock blends: Resilient moduli characteristics. *Constr. Build. Mater.* **2019**, *201*, 207–217. [[CrossRef](#)]
29. Soltani, A.; Taheri, A.; Deng, A.; O’Kelly, B.C. Improved geotechnical behavior of an expansive soil amended with tire-derived aggregates having different gradations. *Minerals* **2020**, *10*, 923. [[CrossRef](#)]
30. ASTM. *Standard Specification for Concrete Aggregates*; ASTM International: West Conshohocken, PA, USA, 2013; C33/C33M;
31. ASTM. *Standard Test Method for Relative Density (Specific Gravity) and Absorption of Fine Aggregate*; ASTM International: West Conshohocken, PA, USA, 2015.
32. ASTM. *Standard Test Methods for Laboratory Determination of Water (Moisture) Content of Soil and Rock by Mass*; ASTM International: West Conshohocken, PA, USA, 2019.
33. ASTM. *Standard Test Methods for Liquid Limit, Plastic Limit, and Plasticity Index of Soils*; ASTM International: West Conshohocken, PA, USA, 2010.
34. ASTM. *Classification of Soils for Engineering Purposes (Unified Soil Classification System)*; American Society of Testing Materials: Philadelphia, PA, USA, 1992.
35. AASHTO. *145-91 Standard Specification for Classification of Soils and Soil-Aggregate Mixtures for Highway Construction Purposes*; American Association of State Highway and Transportation Officials: Washington, DC, USA, 2008.
36. ASTM. *Standard Test Methods for Laboratory Compaction Characteristics of Soil Using Modified Effort (56,000 Ft-lbf/ft³ (2700 KN-m/m³))*; ASTM International: West Conshohocken, PA, USA, 2012; Volume D1557.
37. ASTM. *Test Methods for Specific Gravity of Soil Solids by Water Pycnometer*; ASTM International: West Conshohocken, PA, USA, 2010.
38. ASTM. *Standard Test Methods for Compressive Strength of Molded Soil-Cement Cylinders*; ASTM International: West Conshohocken, PA, USA, 2007.
39. Gnanendran, C.T.; Piratheepan, J. Characterisation of a lightly stabilised granular material by indirect diametrical tensile testing. *Int. J. Pavement Eng.* **2008**, *9*, 445–456. [[CrossRef](#)]
40. Kavussi, A.; Modarres, A. Laboratory fatigue models for recycled mixes with bitumen emulsion and cement. *Constr. Build. Mater.* **2010**, *24*, 1920–1927. [[CrossRef](#)]
41. Thailand Department of Highways. *Standard for Highway Construction (Soil Cement Subbase)*; Thailand Department of Highways: Bangkok, Thailand, 1989; DH-S206/2532;
42. Thailand Department of Highways. *Standard for Highway Construction (Soil Cement Base)*; Thailand Department of Highways: Bangkok, Thailand, 1996; DH-S204/2556;
43. Thailand Department of Highways. *Standard for Highway Construction (Subgrade)*; Thailand Department of Highways: Bangkok, Thailand, 1989; DH-S201/2532;
44. Horpibulsuk, S.; Rachan, R.; Chinkulkijiwat, A.; Raksachon, Y.; Suddeepong, A. Analysis of strength development in cement-stabilized silty clay from microstructural considerations. *Constr. Build. Mater.* **2010**, *24*, 2011–2021. [[CrossRef](#)]
45. Bhuvaneshwari, S.; Robinson, R.; Gandhi, S. Behaviour of lime treated cured expansive soil composites. *Indian Geotech. J.* **2014**, *44*, 278–293. [[CrossRef](#)]
46. Horpibulsuk, S.; Katkan, W.; Sirilerdwattana, W.; Rachan, R. Strength development in cement stabilized low plasticity and coarse grained soils: Laboratory and field study. *Soils Found.* **2006**, *46*, 351–366. [[CrossRef](#)]
47. Sawangsurriya, A.; Bosscher, P.; Edil, T. *Alternative Testing Techniques for Modulus of Pavement Bases and Subgrades*; INDOT Division of Research: West Lafayette, IN, USA, 2005; pp. 108–121.
48. Maley, S.M. *Tire Development for Effective Transportation and Utilization of Used Tires*; CRADA 01-N044 Final Report; National Energy Technology Laboratory: Pittsburgh, PA, USA, 2004.
49. The comptroller General’s Department. *Cost of Construction Materials and Labor Costs 2021*; The Comptroller General’s Department: Bangkok, Thailand, 2021.